Received: 1 February 2025 | Revised: 13 May 2025 | Accepted: 23 July 2025 | Published online: 12 August 2025

RESEARCH ARTICLE

Medinformatics
2025, Vol. 00(00) 1–15
DOI: 10.47852/bonviewMEDIN52025350

BON VIEW PUBLISHING

Repurposing Phytocompounds as JAK1 Inhibitors for Targeting Pancreatic Cancer: A Molecular Docking, ADMET, and MD Simulation Study

Kashif Abbas[1], Mudassir Alam[2,*], Mohsin Hussain[3], Mohd Mustafa[4], Safia Habib[4] and Nazura Usmani[1]

[1]*Department of Zoology, Faculty of Life Sciences, Aligarh Muslim University, India*

[2]*Department of Biological Sciences, Indian Biological Sciences and Research Institute, India*

[3]*Department of Chemical Sciences, University of Naples Federico II, Italy*

[4]*Department of Biochemistry, J.N. Medical College, Aligarh Muslim University, India*

Abstract: The Janus kinase (JAK)/signal transducer and activator of transcription (STAT) pathway plays a central role in the development and advancement of cancer. Janus kinase 1 (JAK1) is essential for the constitutive activation of STAT3, whose activation promotes the development of various cancers including pancreatic ductal adenocarcinoma. This research utilizes computational methods to discover possible phytochemical inhibitors of JAK1 as prospective anticancer treatments. We chose phytochemicals from the Naturally Occurring Plant-based Anti-cancer Compound Activity Target database and evaluated them against JAK1 through molecular docking simulation. Molecular docking showed that tylophorinidine and fisetin exhibited the most favorable docking-based binding strengths, showing scores of −9.9 and −9.1 kcal/mol, respectively. Thorough evaluations involving PASS, ADME/T, drug-likeness, pIC50, and cytotoxicity predictions were performed. Fisetin has surfaced as the leading candidate, demonstrating significant kinase inhibitor potential (Pa = 0.950), advantageous drug-like characteristics, and cytotoxic effects on pancreatic cancer cell lines. Molecular dynamics simulations verified the binding strength of fisetin, with root mean square deviation values consistently approximately 0.25–0.30 nm, similar to the benchmark drug erlotinib. Comprehensive interaction studies showed that fisetin establishes robust interactions with JAK1's binding site, particularly a prominent hydrogen bond with Arg1007. These *in silico* findings suggest that fisetin could serve as a potential natural inhibitor of JAK1 in cancer therapy, highlighting the need for further validation through laboratory and animal-based experiments.

Keywords: JAK1 inhibitors, molecular docking, MD simulation, phytochemicals, pancreatic cancer

1. Introduction

The JAK (Janus-activated kinase) belongs to a family, which comprises non-receptor tyrosine protein kinases [1]. This group of enzymes serves a critical function in several key physiological activities associated with cellular differentiation, growth, metastasis, and programmed cell death in human tissues [2, 3]. JAK1, JAK2, JAK3, and TYK2 represent the four core proteins within the JAK family [4]. JAK3 is specifically expressed in the bone marrow, lymphatic tissues, endothelial cells, and vascular smooth muscle cells, whereas the other JAK family members are broadly distributed across nearly all tissue types [5]. In case of humans, the JAK1 gene can be found on chromosome 1, while JAK2 is located on chromosome 9, and both JAK3 and Tyk2 are situated on chromosome 19 [6]. Structurally, all JAKs are composed of four main domains: an N-terminal FERM domain formed from four-point-one protein, Ezrin, Radixin, and Moesin; an SH2-like domain; a pseudokinase segment known as JH2; and the C-terminal active kinase domain JH1 [7, 8]. The activation of JAKs occurs due to changes in the structure of receptor complexes induced by ligands, triggering a phosphorylation cascade which leads to the activation of the signal transducer and activator of transcription (STAT) family of DNA-binding proteins [9, 10].

Upon close association of receptor-bound JAKs, they undergo activation via transphosphorylation. Once activated, these JAKs add phosphate groups to specific tyrosine residues within the intracellular portion of the cytokine receptor. These phosphorylated residues serve as attachment points for the Src Homology 2 (SH2) domains of STAT proteins. When a STAT protein such as STAT1, STAT2, STAT3, STAT4, STAT5a, STAT5b, or STAT6 binds to the phosphorylated receptor, JAKs further phosphorylate the STAT on a tyrosine residue, triggering its activation. The activated STAT proteins then form dimers and translocate into the nucleus, where they act as transcription factors, regulating the

*Corresponding author: Mudassir Alam, Indian Biological Sciences and Research Institute, India. Email: gh7949@myamu.ac.in

expression of genes involved in cell growth, survival, invasion, and modulation of the immune response [11, 12].

The JAK/STAT pathway plays a significant role in the initiation and advancement of various cancers [13]. Abnormal overactivation of STAT transcription factors has been documented in various hematological malignancies as well as in solid tumors [14], which include various cancer types such as breast [15], lung, liver, and gastric cancers [16–19]. A study reported that JAK1 is crucial for relaying the signals of IL-6 cytokines that exacerbate the advancement of metastatic tumors and promote continuous activation of STAT3 in cancer cells of breast, influenced by the ERBB2 signaling pathway [20, 21]. Studies demonstrated that the dysregulation of the JAK/STAT pathway is commonly observed in various types of cancer. Research has clarified its role in several cellular activities such as migration, apoptosis, and proliferation [22]. Moreover, the aberrant expression and activation elements of the JAK/STAT signaling cascade have been linked with a heightened risk of cancer development [23].

In many of these cancer types, enhanced stimulation of the JAK/STAT pathway correlates with a poorer prognosis, which encompasses a higher likelihood of recurrence and diminished overall survival [24]. Due to the close association between excessive activation of the JAK/STAT pathway and cancer progression and prognosis, STATs and their upstream kinases, JAKs, are being actively explored as potential targets for cancer therapy [25]. Research has shown that mutations in JAK1 have been detected in tumor samples from patients with hepatocellular carcinoma [26], and xenograft models derived from patients harboring the JAK1 S703I mutation showed elevated phosphorylation of STAT3 and STAT5 [27].

In many solid tumors linked to the hyperactivation of STAT3, the progression and development of the disease are associated with either amplified signaling of cytokine or the suppression of negative regulators within the JAK/STAT pathway [28]. In head and neck cancers, aberrant STAT3 activation, often driven by increased IL-6 concentrations in the tumor microenvironment, is associated with accelerated tumor cell growth, resistance to cell death, metastasis, and the suppression of tumor-infiltrating immune cell function [29, 30]. It has been reported that high levels of phosphorylated STAT3 were also detected in gastric tumors compared to healthy tissues [31]. Oncostatin-M, a cytokine from the IL-6 family produced by cancer-associated fibroblasts in NSCLC, activates STAT3 through JAK1 signaling and is implicated in resistance to targeted therapies, including EGFR and MEK inhibitors [32].

The hyperactivation of STAT3 observed in pancreatic cancers, linked to amplified IL-22, induces STAT3 signaling and the suppression of SOCS3, resulting in heightened invasion, migration, and angiogenesis [33, 34]. Although the overactivation of STATs, particularly STAT3, is associated with the emergence and advancement of solid tumors, targeting STATs directly has presented challenges, much like other transcription factors [35]. Consequently, researchers have explored upstream activators of STATs, like JAKs, as possible therapeutic targets in both preclinical and clinical research [36]. Multiple JAK inhibitors have been investigated in the context of solid tumors.

JAK inhibitors represent a category of small-sized chemical inhibitors characterized by distinct chemical configurations [37]. The clinical effectiveness of JAK inhibitors is primarily attributed to two key aspects. First, JAK proteins are essential mediators of various cellular processes. Their inhibition can suppress immune responses and lower the heightened levels of circulating proinflammatory cytokines linked to the JAK/STAT signaling cascade [38]. Second, in certain conditions, like myeloproliferative and cancers, recognizing gain-of-function JAK mutations allows for targeted therapy inhibition [39].

Numerous JAK inhibitors are undergoing investigation in both preclinical and clinical trials. Tofacitinib and baricitinib were the first JAK inhibitors available for oral administration that received approval for rheumatoid arthritis (RA) and other autoimmune diseases [40, 41]. The FDA has approved JAK1/2 selective inhibitor ruxolitinib for treating polycythemia vera, myelofibrosis, and graft versus host disease and has demonstrated a reduction in STAT3 activation in preclinical studies involving various solid tumors. Ruxolitinib has been shown to suppress STAT3 activation and reduce cell proliferation across different types of cancer [42–44]. Drug tofacitinib is another JAK1/3 inhibitor that has received FDA approval for treating RA and ulcerative colitis [45, 46]. In breast cancer models, tofacitinib effectively inhibited STAT3 signaling by restricting its activation and nuclear translocation [47]. In preclinical studies involving prostate tumors, tofacitinib reduced the activation of STAT5 and the process of epithelial to mesenchymal switch [48]. AZD4205 acts as a selective inhibitor of JAK1 [49]. In a preclinical model of NSCLC, administration of AZD4205 led to a reduction in the growth of the tumor and inhibited STAT3 stimulation; these results were more pronounced when AZD4205 was used in conjunction with an EGFR inhibitor such as osimertinib. For instance, a Phase I/II clinical trial has been launched to explore the combination of AZD4205 and osimertinib in patients diagnosed with NSCLC (NCT03450330). The A subunit of chromatin assembly factor 1 has been shown to promote the growth and progression of epithelial ovarian cancer cells through activation of the JAK2/STAT3 signaling cascade. The pan-JAK inhibitor peficitinib reduced cancer growth by blocking this pathway [50].

The *in silico* drug discovery has evolved into a versatile and thorough technique for identifying effective therapeutic agents for various medical conditions. Furthermore, this method is faster and more cost-effective than traditional wet experimental drug development. In the present study, we employed computational approaches to elucidate novel phytochemicals that could serve as drug candidates and inhibitors for JAK1 to treat pancreatic cancer. Our primary hypothesis is that phytochemicals from the Naturally Occurring Plant-based Anti-cancer Compound Activity Target (NPACT) database can effectively bind to and inhibit JAK1, disrupting JAK/STAT signaling cascade in pancreatic cancer cells. We selected phytochemicals from the NPACT database and screened them against JAK1 via molecular docking simulation. Furthermore, drug-likeness properties, pIC50 values, cytotoxic properties against cancer cell lines, PASS analysis, and ADMET profiles of the phytochemicals were evaluated to elucidate their preclinical efficacy. The study aims to identify a lead phytochemical candidate with strong JAK1 inhibitory potential, favorable pharmacokinetic properties, and cytotoxicity against pancreatic cancer cells, providing a foundation for future experimental validation.

2. Material and Methods

2.1. Target selection

The protein target for the study was selected using Therapeutic Target Database (TTD) [51]. TTD is a database that contains information on identified and researched therapeutic targets linked to proteins and nucleic acids, the associated diseases, pathway information, and the particular drugs that target these molecules. JAK1 was selected as the target protein for the study due to its

critical role in the signaling pathways that promote cancer cell growth, survival, and metastasis.

2.2. Selection of phytochemicals

Phytochemicals were retrieved from the NPACT database [52]. Subsequently, ten phytochemicals were selected based on their reported activity against pancreatic cancer, chemical diversity, and availability of structural data in the PubChem database. The selection criteria included evidence of anticancer activity against tumor cell lines from pancreatic tissue or animal models, as documented in NPACT, and the existence of functional groups (e.g., hydroxyl, ketone) known to interact with kinase active sites. Table 1 lists the selected phytochemicals, their chemical names, PubChem IDs, and plant sources, ensuring traceability and relevance to natural product-based drug discovery. The plant sources were cross-referenced with literature and database annotations to confirm their botanical origins.

2.3. Phytochemicals retrieval and their preparation

The aforementioned phytoconstituents were chosen as ligands and retrieved from PubChem in SDF file format. The retrieved ligands underwent preparation for molecular docking with the targeted protein JAK1 using UCSF Chimera 1.15 [53].

2.4. Retrieval of target protein and its processing

The three-dimensional (3D) structure of JAK1 was retrieved from the Protein Data Bank (PDB ID: 6SMB), representing the kinase domain of human JAK1 in complex with a known inhibitor at 2.04 Å and r-value of 0.265. Protein preparation was conducted using PyMOL 3.1 [54, 55]. Non-essential components, including water molecules and heteroatoms (e.g., co-crystallized ligands), were removed to focus on the protein's binding site. Polar hydrogens were added to account for hydrogen bonding potential. Structural optimization was performed using the AMBER ff14SB force field in UCSF Chimera 1.15 [53]. Energy minimization was conducted for 2000 steps using the steepest descent algorithm, followed by 1000 steps of conjugate gradient optimization to relieve steric clashes and optimize bond lengths.

2.5. Screening of phytoconstituents against target protein

Virtual screening of the selected phytochemicals against JAK1 was done using AutoDock Vina [56] integrated within PyRx 0.8 [57]. The JAK1 protein structure (PDB ID: 6SMB) was imported and converted into a macromolecule format. The prepared phytochemical ligand files were converted into pdbqt format using OpenBabel [58] to ensure compatibility with

Table 1. Phytochemicals selected from the NPACT database for molecular docking with targeted protein JAK1

Phytochemical	Structure	Plant source
(r,r)-1,2,4-trihydroxy-16-heptadecene	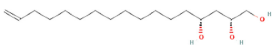	*Persea americana*
1,3-diacetylvilasinin	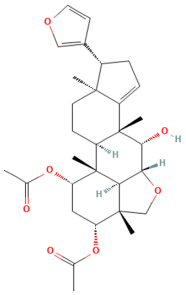	*Azadirachta indica*
Napabucasin	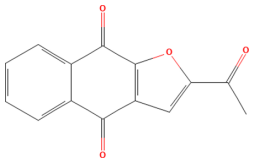	*Ekmanianthe longiflora*
Fisetin	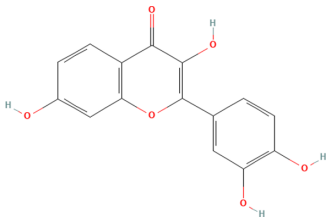	*Fragaria ananassa*
Matrine	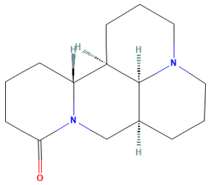	*Sophora flavescens*

(*Continued*)

Table 1. (*Continued*)

Phytochemical	Structure	Plant source
Melianin b	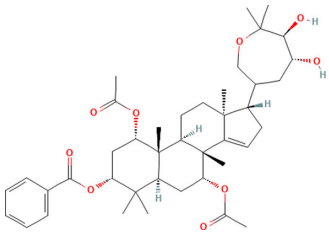	*Melia azedarach*
Meliavolkinin	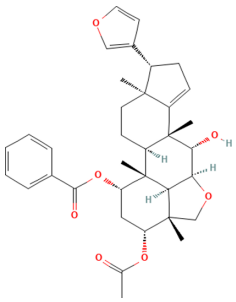	*Melia azedarach*
Naringenin	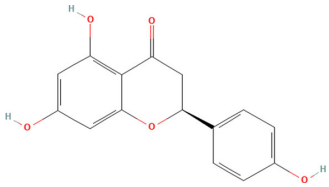	*Citrus sinensis*
Tylophorinidine	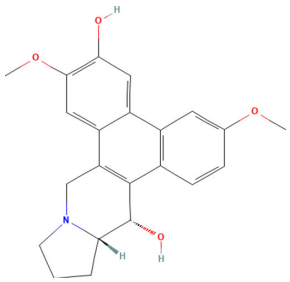	*Tylophora indica*
3'-formyl-2',4',6'-trihydroxy-5'-methyldihydrochalcone	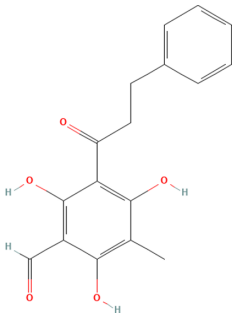	*Psidium guajava*

AutoDock Vina. Subsequently, the docking grid box was configured with dimensions of 58.62 × 52.84 × 54.12 Å, centered at coordinates 13.74, 0.85, and 9.37, to encompass the active site of JAK1. The exhaustiveness parameter was set to 8 to balance computational efficiency and accuracy. To ensure robustness, each docking run was replicated three times, and the pose with the lowest binding energy (highest negative docking score) was selected for further analysis.

2.6. Prediction of activity spectra for substances (PASS) analysis

Biological activity of top-scoring phytocompounds (napabucasin, fisetin, naringenin, tylophorinidine) was evaluated using the Way2Drug PASS web server (https://www.way2drug.com/citation.php) [59]. The phytochemicals were assessed for their potential as kinase inhibitors, focusing on JAK1 inhibition. The

screening threshold was set at Pa > 0.5 (probability of activity) and Pi < 0.05 (probability of inactivity) to identify compounds with a high likelihood of kinase inhibitory activity and low false-positive rates. These thresholds were chosen based on standard practices in computational drug discovery to balance sensitivity and specificity. The Pa and Pi values were calculated for each compound.

2.7. Drug-likeness property of the phytochemicals

The drug-likeness attributes of the phytochemicals were evaluated using the Molsoft web server [60], which calculates the drug-likeness score of the compounds based on their physicochemical characteristics.

2.8. Prediction of cytotoxic property of phytochemicals on cell lines

The anticancer effects of the phytochemicals were estimated in silico using the Cell Line Cytotoxicity Predictor (CLC-Pred) server [61]. CLC-Pred employs a Random Forest machine learning algorithm trained on structural descriptors (e.g., Morgan fingerprints) and cytotoxicity data from human cell lines. For this study, phytochemicals were evaluated for cytotoxicity against pancreatic cancer cell lines, with a focus on the SW1990 cell line, representative of pancreatic ductal adenocarcinoma (PDAC). The simulation method involved putting the SMILES strings of the phytochemicals into CLC-Pred, which generated Pa and Pi values for each compound-cell line pair. A threshold of Pa > 0.3 was used to identify compounds with potential cytotoxic activity, based on the server's validation studies indicating reliable predictions above this cutoff.

2.9. pIC50 value prediction of phytochemicals

A pIC50 value indicates the negative logarithm of the IC50 value of a drug expressed in molar concentration. It acts as a standardized measure of a drug's effectiveness. The pIC50 values of the chosen phytochemicals were calculated using the CODD-Pred server [62].

2.10. ADME/T assessment of phytoconstituents

The analysis of absorption, distribution, metabolism, excretion, and toxicity (ADME/T) was conducted with the Deep-PK server [63]. The ADME/T analysis provides a detailed understanding of a compound's preclinical effectiveness and safety.

2.11. Molecular dynamic simulation

The binding stability between the ligand and the active site of the target protein was analyzed using molecular dynamics (MD) simulation. It was conducted utilizing the WebGro server supplied by the University of Arkansas for Medical Sciences (https://simlab.uams.edu/). Initial molecular topologies were generated using the GlycoBioChemPRODRG2 server. The MD simulations of the complexes were performed using the GROMOS96 43A1 force field combined with the SPC water model, within a triclinic simulation box supplemented with sodium chloride ions. The simulation protocol commenced with energy minimization using the steepest descent method for 5000 steps, followed by equilibration phases under NVT (constant volume and temperature) and NPT (constant pressure and temperature) ensembles, maintained at 300 K and 1 bar. The SPC water model was chosen due to its compatibility with the GROMOS96 43A1 force field, ensuring consistent parameters and reliable solvation behavior. MD simulations were conducted for 50 nanoseconds using the Leap-Frog integrator, constrained by computational resources. The temperature control was achieved using the V rescale thermostat (a modified Berendsen method) set to 300 K with a coupling constant (τ_t) of 0.1 ps, applied every 10 steps. Pressure regulation was managed using the Parrinello-Rahman barostat in isotropic mode, set to 1 bar with a coupling constant (τ_p) of 2 ps and a compressibility of 4.5×10^{-5} bar^{-1}. Simulations employed a 2-femtosecond time step, periodic boundary conditions, and the LINCS algorithm for bond constraints. Extended range electrostatics were computed via the Particle Mesh Ewald (PME) method using a 1.0 nm cutoff, and van der Waals forces were treated with the same cutoff using a potential-shift modifier. PME grid dimensions were set as fourier-nx = 72, fourier-ny = 48, and fourier-nz = 40, with a spacing of 0.16 nm. Accordingly, the approximate simulation box dimensions were calculated as 11.52 nm (x-axis), 7.68 nm (y-axis), and 6.40 nm (z-axis), though actual sizes may vary slightly due to system adjustments. Following equilibration, production runs were carried out with dynamic load balancing enabled to improve computational efficiency. A total of 1000 uniformly spaced frames were extracted from each trajectory for post-simulation analysis. Key structural and dynamic variables, including root mean square deviation (RMSD) and radius of gyration (*Rg*), were computed using the GROMACS 3.0 toolkit to assess the stability and conformational behavior of the complexes at 300 K [64, 65].

2.12. Visualization of interaction between the phytochemicals and the target protein

The two-dimensional and three-dimensional visualization of the protein-ligand interaction was conducted using Discovery Studio 2021 [66] and Pymol 3.1.

3. Result and Discussions

3.1. Virtual screening of the phytochemicals

AutoDock Vina, accessed through PyRx 0.8, was employed to carry out molecular docking studies to assess the binding affinity of ten NPACT-derived phytochemicals to JAK1's kinase domain (PDB ID: 6SMB). Docking scores, reported in kcal/mol, reflect the strength of ligand-protein interactions, with more negative values indicating higher affinity. Table 2 summarizes the results, including PubChem IDs, molecular weights, and docking scores. Tylophorinidine achieved the highest affinity (−9.9 kcal/mol), followed by fisetin (−9.1 kcal/mol), both surpassing erlotinib (−8.5 kcal/mol). Naringenin (−8.7 kcal/mol) and napabucasin (−8.6 kcal/mol) also outperformed erlotinib, validating the docking protocol. The superior scores of tylophorinidine and fisetin suggest strong interactions with JAK1's active site, potentially inhibiting its kinase activity and disrupting JAK/STAT signaling in PDAC cells. Fisetin's high affinity supports the hypothesis by demonstrating that plant-derived compounds can target JAK1 effectively [67]. The docking results prioritize fisetin and tylophorinidine for further analyses, as their affinities indicate potential therapeutic efficacy comparable to or better than erlotinib, a known kinase inhibitor. Tylophorinidine's superior score was unexpected, given its alkaloid structure, but it aligns with the study, which noted alkaloids' high affinity for kinase pockets due to extensive hydrophobic interactions [68].

Table 2. Docking score of various ligands with their PubChem identifiers and molecular weight

Ligands	PubChem ID	Molecular weight (g/mol)	Docking score (kcal/mol)
(R,R)-1,2,4-Trihydroxy-16-heptadecene	21635755	286.4	−5.6
1,3-diacetylvilasinin	52952013	512.6	−7.2
Napabucasin	10331844	240.21	−8.6
Fisetin	5281614	286.24	−9.1
Matrine	91466	248.6	−8.2
Melianin B	44566528	694.9	−7.8
Meliavolkinin	44566525	574.7	−7.3
Naringenin	439246	272.25	−8.7
Tylophorinidine	161749	365.4	−9.9
3'-formyl-2',4',6'-trihydroxy-5'-methyldihydrochalcone	11033908	300.30	−7.8
Erlotinib	176870	393.4	−8.5

3.2. PASS analysis

PASS analysis performed via the Way2Drug server evaluated the kinase inhibitory potential of the top-scoring phytochemicals (tylophorinidine, fisetin, naringenin, napabucasin). PASS uses a Bayesian algorithm to predict biological activity based on structural descriptors, yielding Pa (probability of activity) and Pi (probability of inactivity). A threshold of $Pa > 0.5$ and $Pi < 0.05$ was applied to ensure high specificity for kinase inhibition. Table 3 presents the results. Fisetin exhibited the highest Pa (0.950, $Pi = 0.002$), indicating a strong likelihood of JAK1 inhibition, followed by naringenin ($Pa = 0.838$, $Pi = 0.004$). Napabucasin ($Pa = 0.537$, $Pi = 0.018$) and tylophorinidine ($Pa = 0.552$, $Pi = 0.026$) showed moderate potential. A t-test confirmed fisetin's Pa was significantly higher than tylophorinidine's ($p < 0.01$). The discrepancy between tylophorinidine's high docking score (−9.9 kcal/mol) and moderate Pa may stem from its complex alkaloid structure, which may align less closely with the PASS training set, or lower specificity for JAK1 compared to fisetin's flavonoid scaffold.

3.3. ADME/T analysis

The ADME/T profile of a compound provides insight into the preclinical efficacy of that compound. The ADME/T analysis was performed using the Deep-PK server, and the result of the analysis is given in Table 4. Regarding absorption, napabucasin, fisetin, and naringenin exhibit encouraging profiles with anticipated oral bioavailability and intestinal absorption, whereas tylophorinidine is expected to have no oral bioavailability. All compounds exhibit low skin permeability (log KP > −2.5), which may be important for considerations in topical drug delivery. Importantly, tylophorinidine is anticipated to function as a P-glycoprotein substrate, potentially influencing its absorption and distribution through biological barriers. All compounds exhibit fairly comparable predictions of fraction unbound (spanning from 0.91 to 1.21), indicating similar protein binding traits. The predictions regarding metabolism indicate intricate relationships with cytochrome P450 enzymes. All compounds are anticipated to act as CYP1A2 inhibitors, which may result in possible drug-drug interactions. The compounds exhibit different substrate and inhibitor patterns for other CYP enzymes (2C19, 2C9, 2D6, and 3A4), with each one displaying its own distinct metabolic profile. None of the substances is expected to block OATP1B1 or OATP1B3 transporters. Concerning excretion, all substances exhibit comparable clearance forecasts (7.4–8.89) and are anticipated to possess brief half-lives (<3 h), potentially requiring frequent dosing schedules. None is expected to block the organic cation transporter 2. The toxicity profiles highlight several issues: napabucasin exhibits possible carcinogenic and mutagenic characteristics, and it is also noted for potential respiratory toxicity. Nonetheless, all compounds are expected to be safe concerning different toxicities mediated by nuclear receptors, eye irritation, and toxicity to birds. In conclusion, the evidence indicates that fisetin and naringenin appear to be the most promising options regarding safety. The results may assist in altering structures to enhance pharmacokinetic characteristics while ensuring safety standards remain intact. For example, changes might aim to prolong the half-life of these substances or enhance the oral bioavailability of tylophorinidine while maintaining their advantageous characteristics. Fisetin and naringenin showed favorable oral bioavailability and intestinal absorption, meeting expectations for flavonoids [69].

Table 3. PASS analysis of the phytochemicals using Way2drug server

Ligand	Activity	Pa	Pi
Erlotinib		0.191	0.030
Napabucasin		0.537	0.018
Fisetin	Kinase inhibitor	0.950	0.002
Naringenin		0.838	0.004
Tylophorinidine		0.552	0.026

3.4. Drug-likeness property

Higher positive scores indicate better drug-like characteristics. Figure 1, a high-resolution bar plot, presents the scores. Fisetin achieved the highest score (0.82), followed by tylophorinidine (0.71) and naringenin (0.46). Napabucasin scored negatively (−0.67), indicating poor drug-likeness. Fisetin's high score reflects its optimal molecular weight, lipophilicity, and hydrogen bonding capacity, which makes it appropriate for oral consumption and metabolic stability. These findings support the hypothesis by demonstrating that fisetin possesses drug-like properties conducive to development as a JAK1 inhibitor, enhancing its potential for preclinical studies. The poor score for napabucasin suggests it may require structural modifications, while fisetin's performance aligns with the study's goal of identifying viable natural compounds for PDAC treatment.

Table 4. ADME/T (absorption, distribution, metabolism, excretion, and toxicity) profiles of selected ligands, as analyzed using the Deep-PK server

Parameters	Property	Erlotinib	Napabucasin	Fisetin	Naringenin	Tylophorinidine
Absorption	Human Oral Bioavailability	Bioavailable	Bioavailable	Bioavailable	Bioavailable	Non-Bioavailable
	Human Intestinal Absorption Predictions	Absorbed	Absorbed	Absorbed	Absorbed	Absorbed
	P-Glycoprotein Inhibitor Predictions	Non-Inhibitor	Non-Inhibitor	Non-Inhibitor	Non-Inhibitor	Non-Inhibitor
	P-Glycoprotein Substrate Predictions	Non-Substrate	Non-Substrate	Non-Substrate	Non-Substrate	Substrate
	Skin Permeability Predictions	−3.56	−2.18	−0.55	−1.44	−1.37
	Skin Permeability Interpretation	Low Skin Permeability: log KP > −2.5	Low Skin Permeability: log KP > −2.5	Low Skin Permeability: log KP > −2.5	Low Skin Permeability: log KP > −2.5	Low Skin Permeability: log KP > −2.5
Distribution	Blood-Brain Barrier Predictions	Penetrable	Penetrable	Non-Penetrable	Non-Penetrable	Non-Penetrable
	Fraction Unbound (Human) Predictions	1.11	1.07	0.92	0.91	1.21
Metabolism	CYP 1A2 Inhibitor Predictions	Inhibitor	Inhibitor	Inhibitor	Inhibitor	Inhibitor
	CYP 1A2_substrate Predictions	Substrate	Substrate	Non-Substrate	Substrate	Substrate
	CYP 2C19 Inhibitor Predictions	Non-Inhibitor	Inhibitor	Non-Inhibitor	Inhibitor	Inhibitor
	CYP 2C19_substrate Predictions	Non-Substrate	Substrate	Non-Substrate	Substrate	Non-Substrate
	CYP 2C9 Inhibitor Predictions	Non-Inhibitor	Non-Inhibitor	Inhibitor	Non-Inhibitor	Non-Inhibitor
	CYP 2C9 Substrate Predictions	Non-Substrate	Non-Substrate	Substrate	Substrate	Substrate
	CYP 2D6 Inhibitor Predictions	Inhibitor	Non-Inhibitor	Non-Inhibitor	Non-Inhibitor	Inhibitor
	CYP 2D6 Substrate Predictions	Non-Substrate	Non-Substrate	Non-Substrate	Non-Substrate	Non-Substrate
	CYP 3A4 Inhibitor Predictions	Inhibitor	Non-Inhibitor	Non-Inhibitor	Inhibitor	Non-Inhibitor
	CYP 3A4 Substrate Predictions	Substrate	Non-Substrate	Non-Substrate	Non-Substrate	Non-Substrate
	OATP1B1 Predictions	Non-Inhibitor	Non-Inhibitor	Non-Inhibitor	Non-Inhibitor	Non-Inhibitor
	OATP1B3 Predictions	Non-Inhibitor	Non-Inhibitor	Non-Inhibitor	Non-Inhibitor	Non-Inhibitor
Excretion	Clearance Predictions	8.64	7.5	7.4	8.89	8.53
	Organic Cation Transporter 2 Predictions	Inhibitor	Non-Inhibitor	Non-Inhibitor	Non-Inhibitor	Non-Inhibitor
	Half-Life of Drug Predictions	Half-Life < 3hs	Half-Life < 3hs	Half-Life < 3hs	Half-Life < 3hs	Half-Life < 3hs
Toxicity	AMES Mutagenesis Predictions	Toxic	Toxic	Safe	Safe	Toxic
	Avian Predictions	Safe	Safe	Safe	Safe	Safe
	Bee Predictions	Toxic	Safe	Safe	Toxic	Toxic
	Carcinogenesis Predictions	Safe	Toxic	Safe	Safe	Safe
	Eye Corrosion Predictions	Safe	Safe	Safe	Safe	Safe
	NR-AR Predictions	Safe	Safe	Safe	Safe	Safe
	NR-AR-LBD Predictions	Safe	Safe	Safe	Safe	Safe
	NR-Aromatase Predictions	Toxic	Safe	Safe	Safe	Safe
	NR-GR Predictions	Toxic	Safe	Safe	Safe	Safe
	NR-PPAR-gamma Predictions	Safe	Safe	Safe	Safe	Safe
	Respiratory Disease Predictions	Toxic	Toxic	Safe	Safe	Toxic

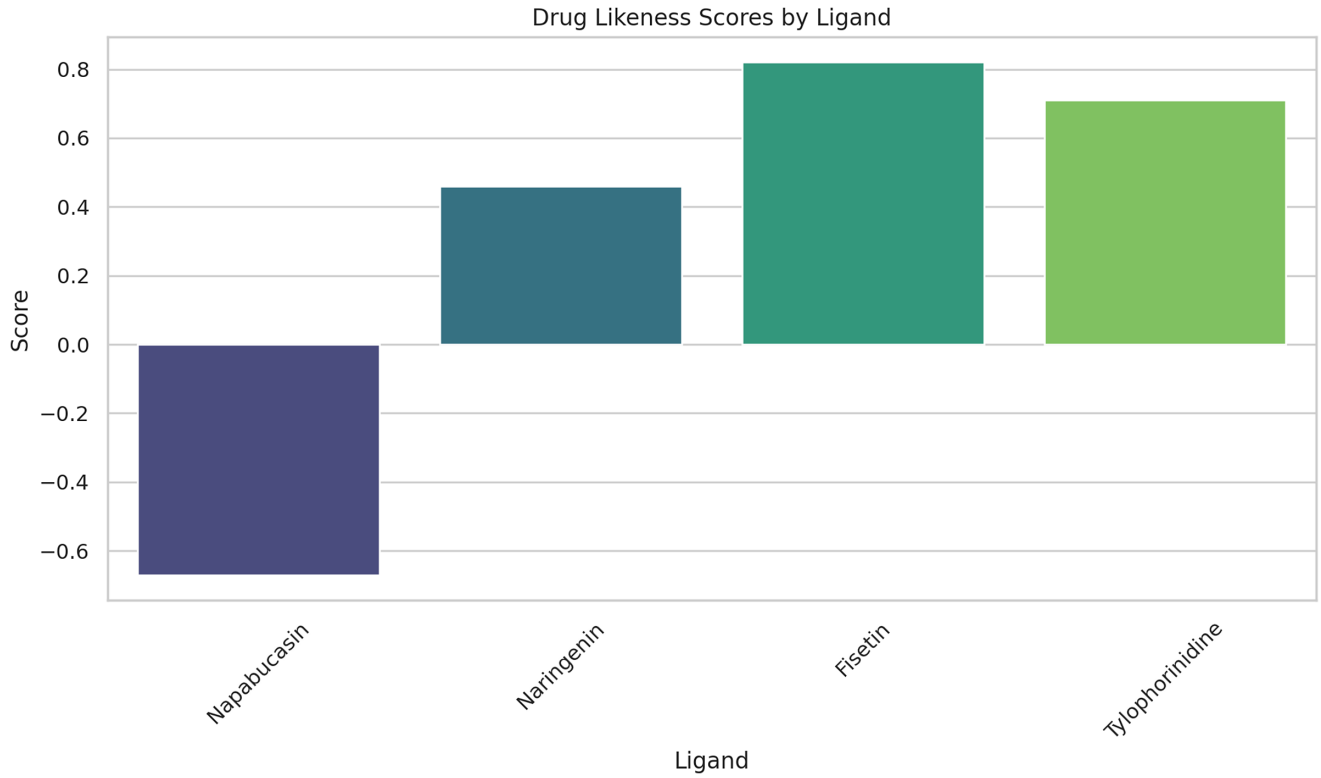

Figure 1. Drug-likeness score of the selected ligands as predicted by Molsoft server

3.5. pIC50 value prediction of phytochemicals

The pIC50 value assists in assessing the biological potency of a substance, especially its ability to inhibit a biological process or target by 50%. It is expressed as the negative logarithm of the IC50 value. This suggests that greater pIC50 values show enhanced potency. Napabucasin, exhibiting a pIC50 of 6.3403, is the most effective compound. Transforming this into IC50 (by computing 10^−6.3403), we obtain roughly 0.457 μM. This indicates that napabucasin needs merely approximately 0.457 micromolar concentration to suppress 50% of the target's function. Fisetin and naringenin exhibit closely matched potencies, with pIC50 values of 6.0580 and 6.0517, translating to IC50 values of approximately 0.876 μM and 0.888 μM. This indicates they require somewhat elevated concentrations compared to napabucasin to reach an equivalent inhibitory effect. Tylophorinidine exhibits the weakest potency with a pIC50 of 5.9201 (IC50 ≈ 1.202 μM), necessitating the greatest concentration among these compounds to reach 50% inhibition. To offer some context, all these substances are quite effective since they function within the low micromolar range. In drug discovery, compounds exhibiting IC50 values in the nanomolar range (pIC50 > 9) are deemed highly effective, whereas those in the low micromolar range (pIC50 > 6) are regarded as promising candidates that may be enhanced via structural alterations.

3.6. Prediction of cytotoxic property of phytochemicals on cell lines

The cytotoxic potential of the phytochemicals against pancreatic cancer cell lines was evaluated using the CLC-Pred server. A threshold of Pa > 0.3 was used to identify significant cytotoxicity. Fisetin was the only compound predicted to have cytotoxic activity against the SW1990 pancreatic cancer cell line (Pa = 0.351, Pi = 0.059), suggesting selective targeting of PDAC cells, potentially via apoptosis or proliferation inhibition. Napabucasin, naringenin, and tylophorinidine showed no significant cytotoxicity (Pa < 0.3). This finding strongly supports the hypothesis, as fisetin's predicted cytotoxicity aligns with its high docking score and PASS probability, indicating both JAK1 inhibition and direct anticancer effects. The SW1990 cell line represents aggressive PDAC, and fisetin's activity against it underscores its therapeutic potential. The lack of cytotoxicity for

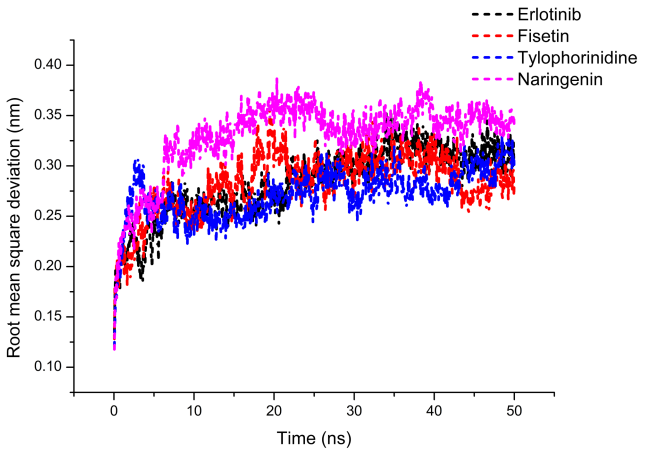

Figure 2. Root mean standard deviation (RMSD) trajectory of complexes for 50 ns MD simulation

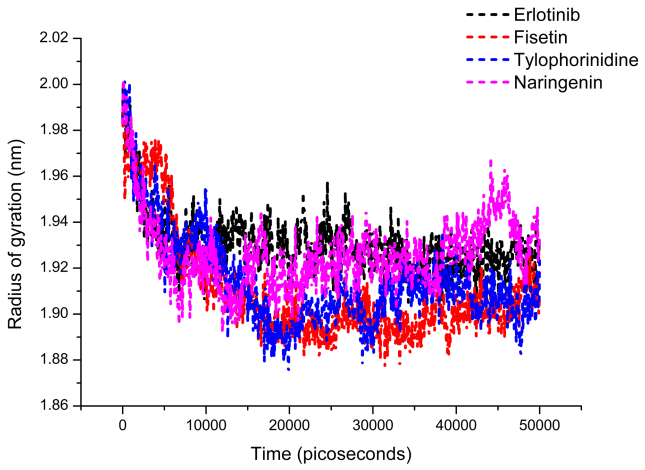

Figure 3. Radius of gyration (Rg) trajectory of complexes for 50 ns MD simulationE

other compounds may reflect limited specificity, highlighting fisetin's unique efficacy.

3.7. Molecular dynamic simulation

RMSD and Rg trajectories were used to examine the stability of the complexes. Napabucasin-JAK1 complex was not used for MD due to its negative drug-likeness score and toxicity profile. Figure 2 depicts the RMSD trajectories for various complexes for 50 ns. Erlotinib was taken as the reference drug. Examining the RMSD trajectory analysis uncovers intriguing details regarding Fisetin's binding stability, illustrated by the red dashed line in the graph. Fisetin exhibits exceptional binding traits with RMSD values consistently hovering around 0.25–0.30 nm following the initial equilibration phase, closely resembling the benchmark drug erlotinib. This similar stability trend is particularly important as it indicates Fisetin might be able to compete with erlotinib's efficacy in inhibiting JAK1. Fisetin is especially intriguing due to its natural source as a flavonoid, along with its proven stability in the JAK1 binding

Table 5. The interaction between the ligands and the active site of the JAK1 protein

Ligand	Interaction	Residues	Bond length (Å)
Fisetin	VDW	Gly882, Glu883, Lys908, Val938, Met956, Phe958, Leu959, Pro960, Gly1020	
	C-H	Gly962	3.55
	Hydrogen	Arg1007	2.67
	Pi-sigma	Leu881	3.61
		Leu889	3.94
		Leu1010	3.63, 3.95
	Pi-alkyl	Leu881	5.30
		Leu889	5.17
		Ala906	4.80, 5.27
Napabucasin	VDW	Gly882, Lys888, Met956, Phe958, Leu959, Gly962, Asn1008, Gly1020, Asp1021	—
	Pi-sigma	Leu881	3.55
		Val889	3.86
		Leu1010	3.65
	Pi-alkyl	Leu881	4.78
		Val889	3.97
		Ala996	4.98
		Leu1010	5.15
Naringenin	VDW	Gly882, Glu882, Gly884, Val938, Met956, Glu957, Phe958, Leu959, Asn1008, Gly1020	
	C-H	Gly962	3.50
	Pi-sigma	Leu881	3.66
		Leu1010	3.64
	Pi-alkyl	Val889	4.54
		Ala906	4.70
Tylophorinidine	VDW	Arg879, Gly882, Glu957, Phe958, Leu959, Pro960, Gly962, Ser963, Glu966, Asp1021	
	C-H	Gly1020	3.48
	Hydrogen	Asn1008	2.35
	Pi-sigma	Leu881	3.96
		Val889	3.77
	Pi-alkyl	Leu881	5.36
		Val889	5.34
		Ala906	3.93, 5.28
		Val938	4.86
		Met956	3.84
		Arg1007	4.27
		Leu1010	3.93, 4.92, 5.34

pocket. The RMSD graph indicates that following the initial equilibration stage (around the first 10 ns), fisetin sustains a consistent trajectory during the rest of the simulation duration. This stability is demonstrated by the steady RMSD values and minor variations, showing that fisetin establishes stable and enduring interactions with the JAK1 binding site. In comparison to naringenin, which demonstrates greater RMSD values (approximately 0.35–0.38 nm) and increased fluctuations, fisetin shows enhanced binding stability, indicating that it might serve as a more dependable JAK1 inhibitor. From a drug development standpoint, these computational results highlight fisetin as a potentially effective natural compound for inhibiting JAK1 in cancer therapy. Its RMSD profile closely reflects that of erlotinib, the recognized reference medication, indicating analogous binding properties and possibly similar inhibitory effects.

The Rg trajectory plot shows the structural compactness of JAK1 complexes with various ligands, including the reference drug erlotinib and three phytochemicals (Figure 3). The Rg values represent how the mass of the complex is distributed relative to its center of mass over the simulation time. Among the tested compounds, naringenin (shown in pink) demonstrates particularly interesting behavior. While all compounds show initial equilibration in the first few nanoseconds, naringenin maintains relatively consistent Rg values throughout the simulation, averaging around 1.92–1.94 nm. More importantly, it shows less fluctuation compared to the reference drug erlotinib (black line), especially in the 30–50 ns range. This suggests that naringenin forms a more stable complex with JAK1, potentially indicating better binding characteristics. When compared with the reference drug erlotinib, both fisetin (red) and tylophorinidine (blue) show slightly lower Rg values (around 1.88–1.90 nm) during the middle phase of the simulation, which might indicate a more compact complex structure.

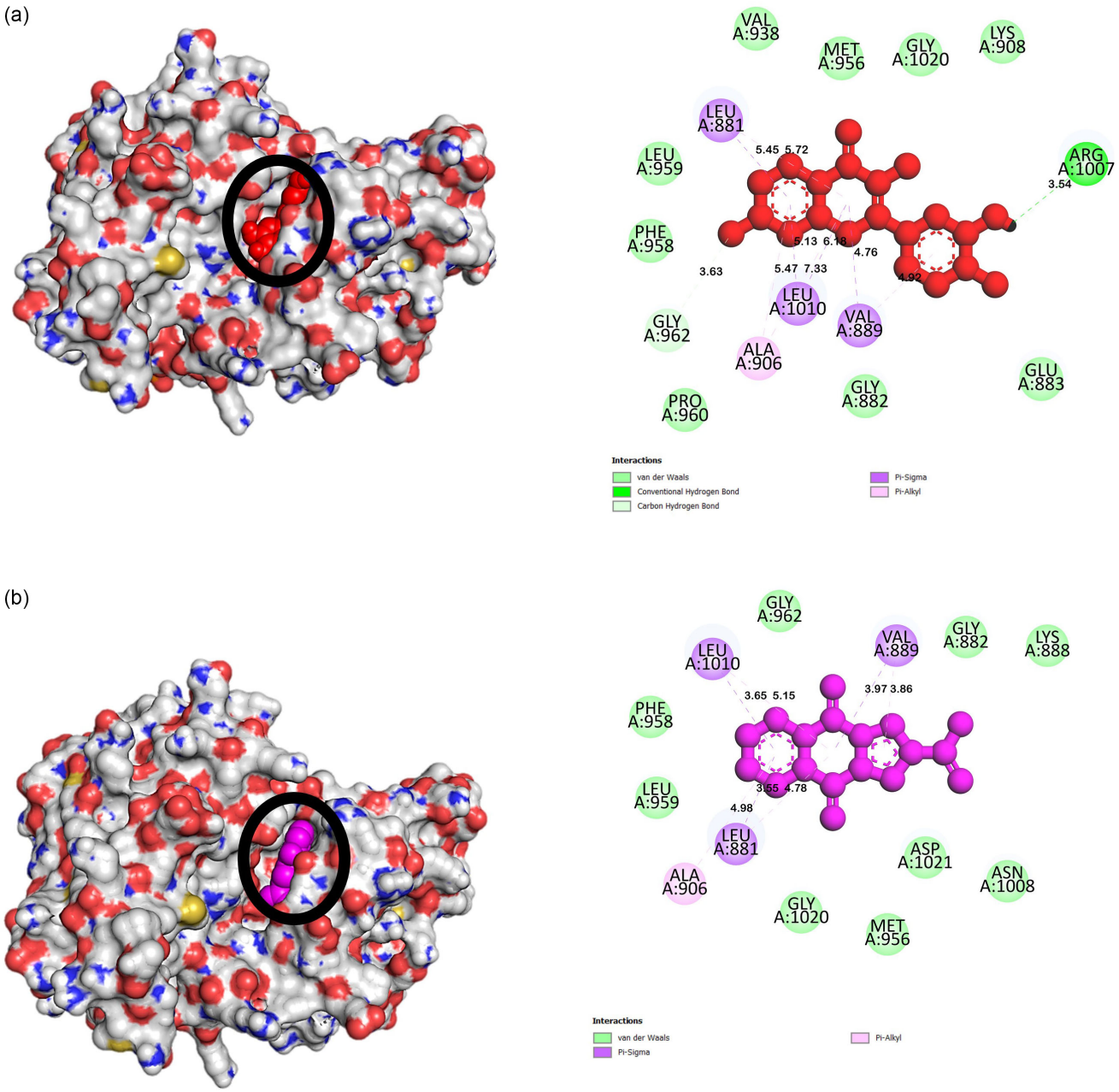

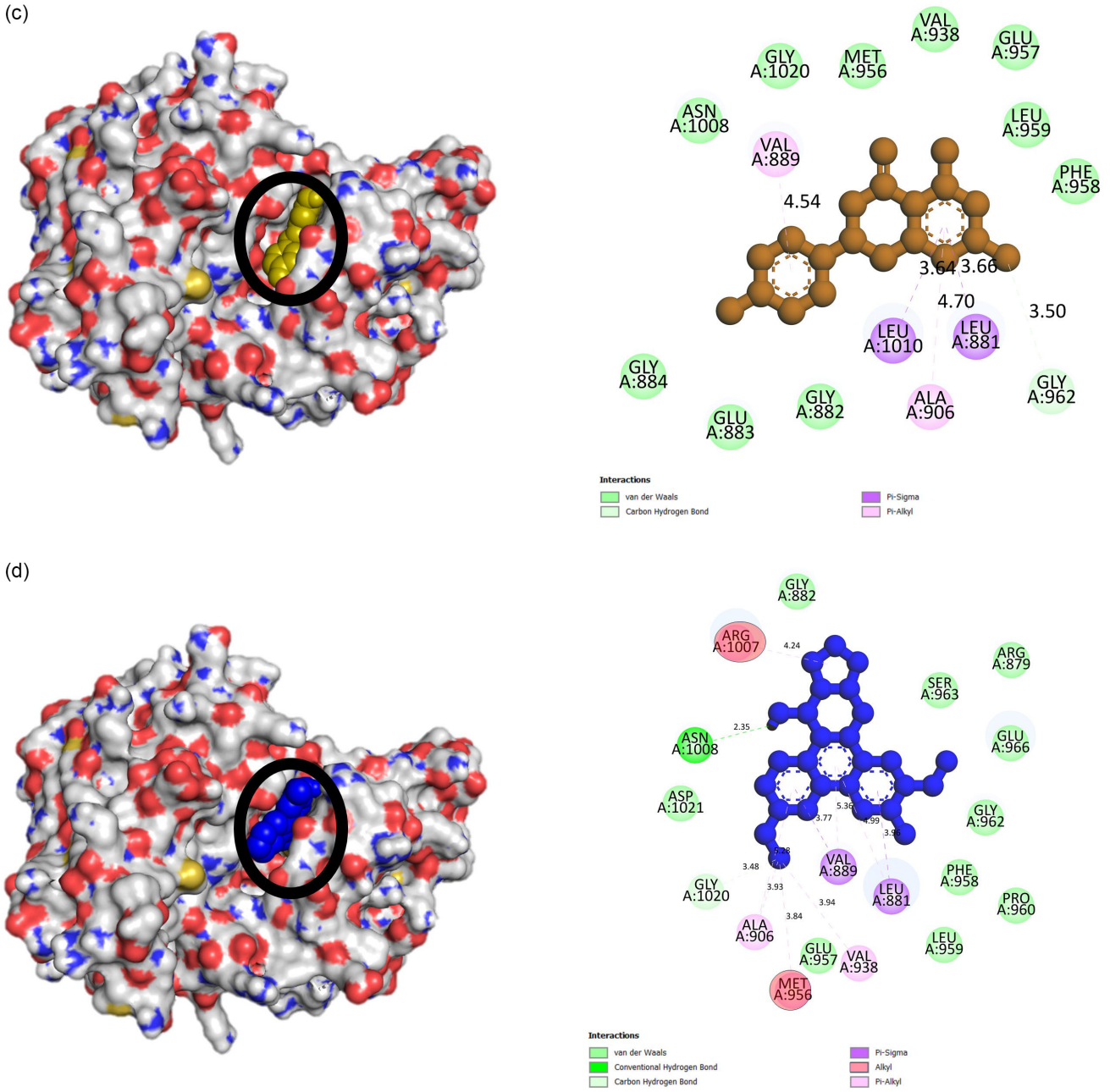

Figure 4. Schematic representation of phytochemicals with active site of JAK1: (a) fisetin, (b) napabucasin, (c) naringenin, and (d) tylophorinidine

3.8. Interaction of ligands with binding pocket of the target protein

The examination of the interaction between ligands and target protein pocket offers information about the ligand's binding potential as well as the interacting residues of the protein's active site (Table 5). Fisetin has a broad interaction profile, indicating considerable binding potential. Its van der Waals (VDW) interactions with nine residues (Gly882, Glu883, Lys908, Val938, Met956, Phe958, Leu959, Pro960, Gly1020) ensure the complex's overall stability. The existence of a hydrogen bond with Arg1007 (2.67 Å) is crucial since hydrogen bonds are stronger than VDW forces. The short bond length (2.67 Å) suggests a strong interaction. Fisetin additionally establishes several pi-sigma interactions with leucine residues (Leu881, Leu889, Leu1010) at distances of 3.61–3.95 Å, as well as pi-alkyl interactions with Leu881, Leu889, and Ala906 at distances of 4.80–5.30 Å. These pi interactions, although less strong than hydrogen bonds, serve a vital function in the overall binding affinity by providing hydrophobic stabilization. Napabucasin demonstrates a somewhat distinct interaction pattern. It creates VDW interactions with nine residues such as Gly882, Lys888, and Met956, among others, ensuring baseline stability. Its pi-sigma interactions with Leu881 (3.55 Å), Val889 (3.86 Å), and Leu1010 (3.65 Å) occur at ideal distances for robust interactions. The pi-alkyl interactions with four residues (Leu881, Val889, Ala996, Leu1010) at distances ranging from 3.97 to 5.15 Å indicate effective hydrophobic stabilization. Significantly, napabucasin does not engage in

hydrogen bonding, potentially leading to a marginally reduced binding affinity when compared to fisetin. Naringenin exhibits a comparatively simple interaction profile. It forms VDW interactions with ten residues, offering extensive yet possibly less potent overall stabilization. It features carbon-hydrogen interaction with Gly962 at 3.50 Å and pi-sigma interactions with Leu881 (3.66 Å) and Leu1010 (3.64 Å). The pi-alkyl interactions with Val889 (4.54 Å) and Ala906 (4.70 Å) occur at greater distances relative to other ligands. The lack of hydrogen bonding and reduced overall interactions may indicate a weaker binding affinity in comparison to fisetin and napabucasin. Tylophorinidine has the most comprehensive interaction network. It has VDW contacts with ten residues, a carbon-hydrogen interaction with Gly1020 (3.48 Å), and a strong hydrogen bond with Asn1008 at 2.35 Å, which is the shortest among all ligands, suggesting a very strong connection. The pi-sigma interactions between Leu881 (3.96 Å) and Val889 (3.77 Å) increase stability, and they exhibit impressive pi-alkyl interactions with eight different residues at distances ranging from 3.84 to 5.36 Å. Figure 4 (a–d) depicts the interactions schematically.

4. Conclusion

This computational analysis offers in-depth perspectives on possible phytochemical JAK1 inhibitors for cancer treatment. Utilizing sophisticated computational methods, we examined and assessed various phytochemicals from the NPACT database, concentrating on their ability to block JAK1, an essential enzyme in cancer development. Fisetin appeared as the most promising candidate, showcasing remarkable traits across various analytical aspects. It demonstrated the greatest potential as a kinase inhibitor, with an activity probability (Pa) of 0.950, and displayed exceptional binding affinity to the JAK1 protein. MD simulations validated its binding stability, as RMSD values closely matched those of the reference drug erlotinib, suggesting possible therapeutic efficacy. The thorough evaluation comprised molecular docking, PASS analysis, ADME/T profiling, and drug-likeness assessment. These computational methods together indicated fisetin's promise as a natural alternative for JAK1 inhibition in cancer therapy. Importantly, its interaction studies showed considerable binding interactions with the JAK1 protein, featuring a strong hydrogen bond with the Arg1007 residue. The research demonstrates the power of computational drug discovery approaches in rapidly and cost-effectively identifying potential anticancer agents targeting the JAK/STAT signaling pathway, offering a valuable preliminary screening method for future therapeutic investigations.

Acknowledgment

The authors would like to acknowledge the Department of Zoology, A.M.U., Aligarh, India; the Indian Biological Sciences and Research Institute, Noida, India; the Department of Chemical Sciences, University of Naples Federico II, Naples, Italy; and the Department of Biochemistry, J.N. Medical College, A.M.U., Aligarh, India, for their invaluable support and contributions.

Ethical Statement

This study does not require any kind of ethical approval as it completely relies on the use of computational techniques and models. This study does not contain any studies with human or animal subjects performed by any of the authors.

Conflicts of Interest

The authors declare that they have no conflicts of interest to this work.

Data Availability Statement

The data that support this work are available upon reasonable request to the corresponding author.

Author Contribution Statement

Kashif Abbas: Conceptualization, Writing – original draft. **Mudassir Alam:** Conceptualization, Resources, Writing – original draft, Project administration. **Mohsin Hussain:** Methodology, Data curation, Writing – original draft. **Mohd Mustafa:** Validation, Visualization. **Safia Habib:** Writing – review & editing, Supervision. **Nazura Usmani:** Investigation, Supervision.

References

[1] Hu, X., Li, J., Fu, M., Zhao, X., & Wang, W. (2021). The JAK/STAT signaling pathway: From bench to clinic. *Signal Transduction and Targeted Therapy*, *6*(1), 402. https://doi.org/10.1038/s41392-021-00791-1

[2] Mengie Ayele, T., Tilahun Muche, Z., Behaile Teklemariam, A., Bogale Kassie, A., & Chekol Abebe, E. (2022). Role of JAK2/STAT3 signaling pathway in the tumorigenesis, chemotherapy resistance, and treatment of solid tumors: A systemic review. *Journal of Inflammation Research*, *15*, 1349–1364. https://doi.org/10.2147/JIR.S353489

[3] Mustafa, M., Ahmad, R., Tantry, I. Q., Ahmad, W., Siddiqui, S., Alam, M., . . . , & Islam, S. (2024). Apoptosis: A comprehensive overview of signaling pathways, morphological changes, and physiological significance and therapeutic implications. *Cells*, *13*(22), 1838. https://doi.org/10.3390/cells13221838

[4] Hu, Q., Bian, Q., Rong, D., Wang, L., Song, J., Huang, H. S., . . . , & Wang, P. Y. (2023). JAK/STAT pathway: Extracellular signals, diseases, immunity, and therapeutic regimens. *Frontiers in Bioengineering and Biotechnology*, *11*, 1110765. https://doi.org/10.3389/fbioe.2023.1110765

[5] Moysidou, G. S., & Dara, A. (2024). JAK inhibition as a potential treatment target in systemic lupus erythematosus. *Mediterranean Journal of Rheumatology*, *35*(Suppl 1), 37–44. https://doi.org/10.31138/mjr.231123.jia

[6] Ziętara, K. J., Wróblewska, K., Zajączkowska, M., Taczała, J., & Lejman, M. (2024). The role of the JAK-STAT pathway in childhood B-cell acute lymphoblastic leukemia. *International Journal of Molecular Sciences*, *25*(13), 6844. https://doi.org/10.3390/ijms25136844

[7] Hosseini, A., Gharibi, T., Marofi, F., Javadian, M., Babaloo, Z., & Baradaran, B. (2020). Janus kinase inhibitors: A therapeutic strategy for cancer and autoimmune diseases. *Journal of Cellular Physiology*, *235*(9), 5903–5924. https://doi.org/10.1002/jcp.29593

[8] Hammarén, H. M., Ungureanu, D., Grisouard, J., Skoda, R. C., Hubbard, S. R., & Silvennoinen, O. (2015). ATP binding to the pseudokinase domain of JAK2 is critical for pathogenic activation. *Proceedings of the National Academy of Sciences of the United States of America*, *112*(15), 4642–4647. https://doi.org/10.1073/pnas.1423201112

[9] Caveney, N. A., Saxton, R. A., Waghray, D., Glassman, C. R., Tsutsumi, N., Hubbard, S. R., & Garcia, K. C. (2023). Structural basis of Janus kinase trans-activation. *Cell Reports*, *42*(3), 112201. https://doi.org/10.1016/j.celrep.2023.112201

[10] Xue, C., Yao, Q., Gu, X., Shi, Q., Yuan, X., Chu, Q., ..., & Li, L. (2023). Evolving cognition of the JAK-STAT signaling pathway: Autoimmune disorders and cancer. *Signal Transduction and Targeted Therapy*, *8*(1), 204. https://doi.org/10.1038/s41392-023-01468-7

[11] Qureshy, Z., Johnson, D. E., & Grandis, J. R. (2020). Targeting the JAK/STAT pathway in solid tumors. *Journal of Cancer Metastasis and Treatment*, *6*, 27. http://dx.doi.org/10.20517/2394-4722.2020.58

[12] Awasthi, N., Liongue, C., & Ward, A. C. (2021). STAT proteins: A kaleidoscope of canonical and non-canonical functions in immunity and cancer. *Journal of Hematology & Oncology*, *14*(1), 198. https://doi.org/10.1186/s13045-021-01214-y

[13] Brooks, A. J., & Putoczki, T. (2020). JAK-STAT signalling pathway in cancer. *Cancers*, *12*(7), 1971. https://doi.org/10.3390/cancers12071971

[14] Tolomeo, M., & Cascio, A. (2021). The multifaced role of STAT3 in cancer and its implication for anticancer therapy. *International Journal of Molecular Sciences*, *22*(2), 603. https://doi.org/10.3390/ijms22020603

[15] Sathish, S., Sohn, H., & Madhavan, T. (2025). An In Silico approach to uncover selective JAK1 inhibitors for breast cancer from life chemicals database. *Applied Biochemistry and Biotechnology*. Advance online publication. https://doi.org/10.1007/s12010-024-05109-9

[16] Xiong, A., Yang, Z., Shen, Y., Zhou, J., & Shen, Q. (2014). Transcription factor STAT3 as a novel molecular target for cancer prevention. *Cancers*, *6*(2), 926–957. https://doi.org/10.3390/cancers6020926

[17] Parakh, S., Ernst, M., & Poh, A. R. (2021). Multicellular effects of STAT3 in non-small cell lung cancer: Mechanistic insights and therapeutic opportunities. *Cancers*, *13*(24), 6228. https://doi.org/10.3390/cancers13246228

[18] Geiger, J. L., Grandis, J. R., & Bauman, J. E. (2016). The STAT3 pathway as a therapeutic target in head and neck cancer: Barriers and innovations. *Oral Oncology*, *56*, 84–92. https://doi.org/10.1016/j.oraloncology.2015.11.022

[19] Yadav, P., Azram, M., Faraz, M., Alam, M., & Khan, S. (2025). In Silico screening of Rauwolfia Serpentina phytochemicals as orexin receptor-2 agonists for the management of narcolepsy. *International Journal of Biochemistry Research & Review*, *34*(1), 76–102. https://doi.org/10.9734/ijbcrr/2025/v34i1951

[20] Wehde, B. L., Rädler, P. D., Shrestha, H., Johnson, S. J., Triplett, A. A., & Wagner, K. U. (2018). Janus Kinase 1 plays a critical role in mammary cancer progression. *Cell Reports*, *25*(8), 2192–2207.e5. https://doi.org/10.1016/j.celrep.2018.10.063

[21] Hawthorne, V. S., Huang, W. C., Neal, C. L., Tseng, L. M., Hung, M. C., & Yu, D. (2009). ErbB2-mediated Src and signal transducer and activator of transcription 3 activation leads to transcriptional up-regulation of p21Cip1 and chemoresistance in breast cancer cells. *Molecular Cancer Research: MCR*, *7*(4), 592–600. https://doi.org/10.1158/1541-7786.MCR-08-0316

[22] Rah, B., Rather, R. A., Bhat, G. R., Baba, A. B., Mushtaq, I., Farooq, M., ..., & Afroze, D. (2022). JAK/STAT signaling: Molecular targets, therapeutic opportunities, and limitations of targeted inhibitions in solid malignancies. *Frontiers in Pharmacology*, *13*, 821344. https://doi.org/10.3389/fphar.2022.821344

[23] Gutiérrez-Hoya, A., & Soto-Cruz, I. (2020). Role of the JAK/STAT pathway in cervical cancer: Its relationship with HPV E6/E7 oncoproteins. *Cells*, *9*(10), 2297. https://doi.org/10.3390/cells9102297

[24] Pencik, J., Pham, H. T., Schmoellerl, J., Javaheri, T., Schlederer, M., Culig, Z., ..., & Kenner, L. (2016). JAK-STAT signaling in cancer: From cytokines to non-coding genome. *Cytokine*, *87*, 26–36. https://doi.org/10.1016/j.cyto.2016.06.017

[25] Kohal, R., Bisht, P., Gupta, G. D., & Verma, S. K. (2024). Targeting JAK2/STAT3 for the treatment of cancer: A review on recent advancements in molecular development using structural analysis and SAR investigations. *Bioorganic Chemistry*, *143*, 107095. https://doi.org/10.1016/j.bioorg.2023.107095

[26] Yang, S., Luo, C., Gu, Q., Xu, Q., Wang, G., Sun, H., ..., & Fang, D. D. (2016). Activating JAK1 mutation may predict the sensitivity of JAK-STAT inhibition in hepatocellular carcinoma. *Oncotarget*, *7*(5), 5461–5469. https://doi.org/10.18632/oncotarget.6684

[27] Kan, Z., Zheng, H., Liu, X., Li, S., Barber, T. D., Gong, Z., ..., & Mao, M. (2013). Whole-genome sequencing identifies recurrent mutations in hepatocellular carcinoma. *Genome Research*, *23*(9), 1422–1433. https://doi.org/10.1101/gr.154492.113

[28] Igelmann, S., Neubauer, H. A., & Ferbeyre, G. (2019). STAT3 and STAT5 activation in solid cancers. *Cancers*, *11*(10), 1428. https://doi.org/10.3390/cancers11101428

[29] Wang, Y., Wu, C., Zhang, C., Li, Z., Zhu, T., Chen, J., ..., & Zhou, X. (2018). TGF-β-induced STAT3 overexpression promotes human head and neck squamous cell carcinoma invasion and metastasis through malat1/miR-30a interactions. *Cancer Letters*, *436*, 52–62. https://doi.org/10.1016/j.canlet.2018.08.009

[30] Bu, L. L., Yu, G. T., Wu, L., Mao, L., Deng, W. W., Liu, J. F., ..., & Sun, Z. J. (2017). STAT3 induces immunosuppression by upregulating PD-1/PD-L1 in HNSCC. *Journal of Dental Research*, *96*(9), 1027–1034. https://doi.org/10.1177/0022034517712435

[31] Chen, M., Wang, T., Tian, D., Hai, C., & Qiu, Z. (2024). Induction, growth, drug resistance, and metastasis: A comprehensive summary of the relationship between STAT3 and gastric cancer. *Heliyon*, *10*(18), e37263. https://doi.org/10.1016/j.heliyon.2024.e37263

[32] Shien, K., Papadimitrakopoulou, V. A., Ruder, D., Behrens, C., Shen, L., Kalhor, N., ..., & Izzo, J. G. (2017). JAK1/STAT3 activation through a proinflammatory cytokine pathway leads to resistance to molecularly targeted therapy in non-small cell lung cancer. *Molecular Cancer Therapeutics*, *16*(10), 2234–2245. https://doi.org/10.1158/1535-7163.MCT-17-0148

[33] He, W., Wu, J., Shi, J., Huo, Y. M., Dai, W., Geng, J., ..., & Xue, J. (2018). IL22RA1/STAT3 signaling promotes stemness and tumorigenicity in pancreatic cancer. *Cancer Research*, *78*(12), 3293–3305. https://doi.org/10.1158/0008-5472.CAN-17-3131

[34] Lin, X. M., Chen, H., & Zhan, X. L. (2019). MiR-203 regulates JAK-STAT pathway in affecting pancreatic cancer cells proliferation and apoptosis by targeting SOCS3. *European Review for Medical and Pharmacological Sciences*, *23*(16), 6906–6913. https://doi.org/10.26355/eurrev_201908_18730

[35] Tošić, I., & Frank, D. A. (2021). STAT3 as a mediator of oncogenic cellular metabolism: Pathogenic and therapeutic implications. *Neoplasia (New York, N.Y.)*, *23*(12), 1167–1178. https://doi.org/10.1016/j.neo.2021.10.003

[36] Tabassum, S., Abbasi, R., Ahmad, N., & Farooqi, A. A. (2019). Targeting of JAK-STAT signaling in breast cancer: Therapeutic strategies to overcome drug resistance. *Advances in Experimental Medicine and Biology*, *1152*, 271–281. https://doi.org/10.1007/978-3-030-20301-6_14

[37] Wei, X. H., & Liu, Y. Y. (2024). Potential applications of JAK inhibitors, clinically approved drugs against autoimmune diseases, in cancer therapy. *Frontiers in Pharmacology*, *14*, 1326281. https://doi.org/10.3389/fphar.2023.1326281

[38] Sarapultsev, A., Gusev, E., Komelkova, M., Utepova, I., Luo, S., & Hu, D. (2023). JAK-STAT signaling in inflammation and stress-related diseases: Implications for therapeutic interventions. *Molecular Biomedicine*, *4*(1), 40. https://doi.org/10.1186/s43556-023-00151-1

[39] Li, B., Rampal, R. K., & Xiao, Z. (2019). Targeted therapies for myeloproliferative neoplasms. *Biomarker Research*, *7*, 15. https://doi.org/10.1186/s40364-019-0166-y

[40] Taylor P. C. (2019). Clinical efficacy of launched JAK inhibitors in rheumatoid arthritis. *Rheumatology (Oxford, England)*, *58*(Suppl 1), i17–i26. https://doi.org/10.1093/rheumatology/key225

[41] Shawky, A. M., Almalki, F. A., Abdalla, A. N., Abdelazeem, A. H., & Gouda, A. M. (2022). A comprehensive overview of globally approved JAK inhibitors. *Pharmaceutics*, *14*(5), 1001. https://doi.org/10.3390/pharmaceutics14051001

[42] Lu, C., Talukder, A., Savage, N. M., Singh, N., & Liu, K. (2017). JAK-STAT-mediated chronic inflammation impairs cytotoxic T lymphocyte activation to decrease anti-PD-1 immunotherapy efficacy in pancreatic cancer. *Oncoimmunology*, *6*(3), e1291106. https://doi.org/10.1080/2162402X.2017.1291106

[43] Vannucchi, A. M., Verstovsek, S., Guglielmelli, P., Griesshammer, M., Burn, T. C., Naim, A., …, & Kiladjian, J. J. (2017). Ruxolitinib reduces JAK2 p.V617F allele burden in patients with polycythemia vera enrolled in the RESPONSE study. *Annals of Hematology*, *96*(7), 1113–1120. https://doi.org/10.1007/s00277-017-2994-x

[44] Qureshy, Z., Li, H., Zeng, Y., Rivera, J., Cheng, N., Peterson, C. N., …, & Grandis, J. R. (2022). STAT3 activation as a predictive biomarker for ruxolitinib response in head and neck cancer. *Clinical Cancer Research: An Official Journal of the American Association for Cancer Research*, *28*(21), 4737–4746. https://doi.org/10.1158/1078-0432.CCR-22-0744

[45] Virtanen, A. T., Haikarainen, T., Raivola, J., & Silvennoinen, O. (2019). Selective JAKinibs: Prospects in inflammatory and autoimmune diseases. *BioDrugs: Clinical Immunotherapeutics, Biopharmaceuticals and Gene Therapy*, *33*(1), 15–32. https://doi.org/10.1007/s40259-019-00333-w

[46] Alam, M., Abbas, K., Mustafa, M., Usmani, N., & Habib, S. (2024). Microbiome-based therapies for Parkinson's disease. *Frontiers in Nutrition*, *11*, 1496616. https://doi.org/10.3389/fnut.2024.1496616

[47] Lapeire, L., Hendrix, A., Lambein, K., Van Bockstal, M., Braems, G., Van Den Broecke, R., …, & De Wever, O. (2014). Cancer-associated adipose tissue promotes breast cancer progression by paracrine oncostatin M and Jak/STAT3 signaling. *Cancer Research*, *74*(23), 6806–6819. https://doi.org/10.1158/0008-5472.CAN-14-0160

[48] Seol, M. A., Kim, J. H., Oh, K., Kim, G., Seo, M. W., Shin, Y. K., …, & Kim, H. R. (2019). Interleukin-7 contributes to the invasiveness of prostate cancer cells by promoting epithelial-mesenchymal transition. *Scientific Reports*, *9*(1), 6917. https://doi.org/10.1038/s41598-019-43294-4

[49] Su, Q., Banks, E., Bebernitz, G., Bell, K., Borenstein, C. F., Chen, H., …, & Kettle, J. G. (2020). Discovery of (2R)-N-[3-[2-[(3-Methoxy-1-methyl-pyrazol-4-yl)amino]pyrimidin-4-yl]-1H-indol-7-yl]-2-(4-methylpiperazin-1-yl)propenamide (AZD4205) as a potent and selective Janus Kinase 1 inhibitor. *Journal of Medicinal Chemistry*, *63*(9), 4517–4527. https://doi.org/10.1021/acs.jmedchem.9b01392

[50] Xia, D., Xu, X., Wei, J., Wang, W., Xiong, J., Tan, Q., …, & Wang, H. (2023). CHAF1A promotes the proliferation and growth of epithelial ovarian cancer cells by affecting the phosphorylation of JAK2/STAT3 signaling pathway. *Biochemistry and Biophysics Reports*, *35*, 101522. https://doi.org/10.1016/j.bbrep.2023.101522

[51] Zhou, Y., Zhang, Y., Zhao, D., Yu, X., Shen, X., Zhou, Y., …, & Zhu, F. (2024). TTD: Therapeutic target database describing target druggability information. *Nucleic Acids Research*, *52*(D1), D1465–D1477. https://doi.org/10.1093/nar/gkad751

[52] Mangal, M., Sagar, P., Singh, H., Raghava, G. P., & Agarwal, S. M. (2013). NPACT: Naturally occurring plant-based anti-cancer compound-activity-target database. *Nucleic Acids Research*, *41*(Database issue), D1124–D1129. https://doi.org/10.1093/nar/gks1047

[53] Butt, S. S., Badshah, Y., Shabbir, M., & Rafiq, M. (2020). Molecular docking using Chimera and AutoDock Vina software for nonbioinformaticians. *JMIR Bioinformatics and Biotechnology*, *1*(1), e14232. https://doi.org/10.2196/14232

[54] Yuan, S., Chan, H. S., & Hu, Z. (2017). Using PyMOL as a platform for computational drug design. *Wiley Interdisciplinary Reviews: Computational Molecular Science*, *7*(2), e1298. https://doi.org/10.1002/wcms.1298

[55] Rosignoli, S., & Paiardini, A. (2022). Boosting the full potential of PyMOL with structural biology plugins. *Biomolecules*, *12*(12), 1764. https://doi.org/10.3390/biom12121764

[56] Trott, O., & Olson, A. J. (2010). AutoDock Vina: Improving the speed and accuracy of docking with a new scoring function, efficient optimization, and multithreading. *Journal of Computational Chemistry*, *31*(2), 455–461. https://doi.org/10.1002/jcc.21334

[57] Alamri, M. A., & Alamri, M. A. (2019). Pharmacophore and docking-based sequential virtual screening for the identification of novel Sigma 1 receptor ligands. *Bioinformation*, *15*(8), 586–595. https://doi.org/10.6026/97320630015586

[58] O'Boyle, N. M., Banck, M., James, C. A., Morley, C., Vandermeersch, T., & Hutchison, G. R. (2011). Open Babel: An open chemical toolbox. *Journal of Cheminformatics*, *3*, 33. https://doi.org/10.1186/1758-2946-3-33

[59] Filimonov, D. A., Rudik, A. V., Dmitriev, A. V., & Poroikov, V. V. (2020). Computer-aided estimation of biological activity profiles of drug-like compounds taking into account their metabolism in human body. *International Journal of Molecular Sciences*, *21*(20), 7492. https://doi.org/10.3390/ijms21207492

[60] Sri Prakash, S. R., Kamalnath, S. M., Antonisamy, A. J., Marimuthu, S., & Malayandi, S. (2023). In Silico molecular docking of phytochemicals for type 2 diabetes mellitus therapy: A network pharmacology approach. *International Journal of Molecular and Cellular Medicine*, *12*(4), 372–387. https://doi.org/10.22088/IJMCM.BUMS.12.4.372

[61] Lagunin, A. A., Rudik, A. V., Pogodin, P. V., Savosina, P. I., Tarasova, O. A., Dmitriev, A. V., …, & Poroikov, V. V. (2023). CLC-Pred 2.0: A freely available web application for

In Silico prediction of human cell line cytotoxicity and molecular mechanisms of action for druglike compounds. *International Journal of Molecular Sciences*, *24*(2), 1689. https://doi.org/10.3390/ijms24021689

[62] Yin, X., Wang, X., Li, Y., Wang, J., Wang, Y., Deng, Y., . . . , & Yao, X. (2023). CODD-Pred: A web server for efficient target identification and bioactivity prediction of small molecules. *Journal of Chemical Information and Modeling*, *63*(20), 6169–6176. https://doi.org/10.1021/acs.jcim.3c00685

[63] Myung, Y., de Sá, A. G. C., & Ascher, D. B. (2024). Deep-PK: Deep learning for small molecule pharmacokinetic and toxicity prediction. *Nucleic Acids Research*, *52*(W1), W469–W475. https://doi.org/10.1093/nar/gkae254

[64] Zolghadr, L., Behbehani, G. R., PakBin, B., Hosseini, S. A., Divsalar, A., & Gheibi, N. (2022). Molecular dynamics simulations, molecular docking, and kinetics study of kaempferol interaction on Jack bean urease: Comparison of extended solvation model. *Food Science & Nutrition*, *10*(11), 3585–3597. https://doi.org/10.1002/fsn3.2956

[65] Hirano, Y., Okimoto, N., Fujita, S., & Taiji, M. (2021). Molecular dynamics study of conformational changes of Tankyrase 2 binding subsites upon ligand binding. *ACS Omega*, *6*(27), 17609–17620. https://doi.org/10.1021/acsomega.1c02159

[66] Prasada Rao, C. M., Silakabattini, K., Narapusetty, N., Marabathuni, V. J. P., Thejomoorthy, K., Rajeswari, T., & Y, S. (2023). Insights from the molecular docking and simulation analysis of P38 MAPK phytochemical inhibitor complexes. *Bioinformation*, *19*(3), 323–330. https://doi.org/10.6026/97320630019323

[67] Kubina, R., Krzykawski, K., Kabała-Dzik, A., Wojtyczka, R. D., Chodurek, E., & Dziedzic, A. (2022). Fisetin, a potent anticancer flavonol exhibiting cytotoxic activity against neoplastic malignant cells and cancerous conditions: A scoping, comprehensive review. *Nutrients*, *14*(13), 2604. https://doi.org/10.3390/nu14132604

[68] Vergoten, G., & Bailly, C. (2024). Interaction of Norsecurinine-Type oligomeric alkaloids with α-Tubulin: A molecular docking study. *Plants*, *13*(9), 1269. https://doi.org/10.3390/plants13091269

[69] Hu, L., Luo, Y., Yang, J., & Cheng, C. (2025). Botanical flavonoids: Efficacy, absorption, metabolism and advanced pharmaceutical technology for improving bioavailability. *Molecules*, *30*(5), 1184. https://doi.org/10.3390/molecules30051184

How to Cite: Abbas, K., Alam, M., Hussain, M., Mustafa, M., Habib, S., & Usmani, N. (2025). Repurposing Phytocompounds as JAK1 Inhibitors for Targeting Pancreatic Cancer: A Molecular Docking, ADMET, and MD Simulation Study. *Medinformatics*. https://doi.org/10.47852/bonviewMEDIN52025350